Isothermal structural transitions, magnetization and large piezoelectric response in $Bi_{1-x}La_xFeO_3$ perovskites

I. O. Troyanchuk,[1,*] D. V. Karpinsky,[1,2] M. V. Bushinsky,[1] V. A. Khomchenko,[3] G. N. Kakazei,[4,5] J. P. Araujo,[4] M. Tovar,[6] V. Sikolenko,[7,8] V. Efimov,[7] and A. L. Kholkin[2]

[1]*Scientific-Practical Materials Research Centre (SSPA) of NAS of Belarus, P. Brovka str. 19, BY-220072 Minsk, Belarus*
[2]*CICECO/Department of Ceramics and Glass Engineering, University of Aveiro, PT-3810-193 Aveiro, Portugal*
[3]*CEMDRX/Department of Physics, Faculty of Sciences and Technology, University of Coimbra, PT-3004-516 Coimbra, Portugal*
[4]*IFIMUP/Department of Physics, Faculty of Sciences, University of Porto, PT-4169-007 Porto, Portugal*
[5]*Institute of Magnetism, NAS of Ukraine, 36 b Vernadskogo Boulevard, UA-03142 Kiev, Ukraine*
[6]*Helmholtz-Zentrum-Berlin for Materials and Energy, DE-14109 Berlin, Germany*
[7]*Joint Institute for Nuclear Research, Dubna, RU-141980 Russia*
[8]*Paul Scherrer Institute, CH-5232 Villigen, Switzerland*

(Received 27 October 2010; revised manuscript received 12 January 2011; published 22 February 2011)

We report on the discovery of an isothermal structural transition observed in $Bi_{1-x}La_xFeO_3$ ($0.17 \leqslant x \leqslant 0.19$) ceramics. At room temperature, an initially pure polar rhombohedral phase gradually transforms into a pure antipolar orthorhombic one. The polar phase can be recovered by annealing at $T > 300\,^{\circ}C$. In accordance with neutron powder diffraction data, an inverse isothermal antipolar-polar transition takes place at $T > 300\,^{\circ}C$, where the polar phase becomes more stable. The antipolar phase is characterized by a weak ferromagnetic state, whereas the polar phase has been obtained in a mixed antiferromagnet–weak ferromagnet state. The relatively low external pressure induces polar-antipolar transition, but there is no evidence of electric-field-driven antipolar-polar transition. The observed large local piezoelectric response is associated with structural instability of the polar phase, whereas local multistate piezoelectric loops can be related to the domain wall pinning effect.

DOI: 10.1103/PhysRevB.83.054109 PACS number(s): 61.05.cp, 75.30.Cr, 77.65.Bn, 64.70.kp

I. INTRODUCTION

$BiFeO_3$ is a very rare example of a single-phase material in which ferroelectricity, antiferromagnetism, and ferroelasticity coexist in a broad temperature range.[1] High transition temperatures and a large spontaneous polarization make this compound a good candidate for various device applications.[1] Intriguing behavior was recently found in lanthanide-substituted compounds.[2–7] Namely, double polarization hysteresis loops and enhanced piezoelectric activity (up to 110 pm/V, compared with 60 pm/V for parent $BiFeO_3$) were revealed in Sm-doped thin films at the phase boundary of a rhombohedral-to-orthorhombic phase transition.[2,3] A similar structural transition was also observed in ceramic samples of the $Bi_{1-x}Nd_xFeO_3$ system around $x = 0.15$.[4–6] Crystal structure refinement showed that the $Bi_{0.85}Nd_{0.15}FeO_3$ possessed an antipolar orthorhombic structure (the space group *Pbam* can be used as a first approximation to describe the structure of the room-temperature phase), which transforms into nonpolar *Pnma* on heating slightly above $300\,^{\circ}C$.[4–6] The origin of the double hysteresis loops and corresponding enhancement of the piezoelectric properties of $Bi_{1-x}Sm_xFeO_3$ thin films was discussed in terms of the electric-field-induced transition from a nonpolar orthorhombic (*Pnma*) to a polar rhombohedral (*R3c*) phase.[7]

Taking into account the results of recent research,[2–7] we decided to reinvestigate the $Bi_{1-x}La_xFeO_3$ system in a broad range of lanthanum concentrations. In previous studies, it was reported that $x \leqslant 0.15$ compounds possessed a polar structure (space group *R3c*).[8,9] For higher lanthanum concentrations, data on structural state and physical properties of the system were contradictory,[6,9–11] because the sample preparation procedure was not optimized. In this paper, we report on the striking structural, magnetic, and piezoelectric behavior observed in $Bi_{1-x}La_xFeO_3$ multiferroics near the polar-antipolar phase boundary.

II. EXPERIMENTAL

Ceramic samples of $Bi_{1-x}La_xFeO_3$ ($x = 0$, $0.16 \lesssim x \lesssim 0.5$) were prepared by a solid-state reaction technique using the high-purity oxides Bi_2O_3, La_2O_3, and Fe_2O_3 taken in a stoichiometric ratio and thoroughly mixed using a planetary mill (Retsch). Pure $BiFeO_3$ was synthesized at $870\,^{\circ}C$ for 10 min. Doped compounds were prepared at 950–$1040\,^{\circ}C$ for 15 h (synthesis temperature was increased with increasing lanthanum content).

X-ray diffraction (XRD) patterns were collected at room temperature using a DRON-3M diffractometer with CuK_α radiation. Neutron diffraction data were obtained using a high-resolution neutron powder diffractometer E9 (Firepod) at the Berlin Neutron Scattering Center (BENSC) of Helmholtz-Zentrum Berlin (HZB). A neutron beam with a wavelength of 1.7977 Å was generated from a Ge (511) monochromator. The crystal and magnetic structures were analyzed by the Rietveld method using the FullProf program.[12]

Local ferroelectric properties were investigated with piezoresponse force microscopy (PFM) using a commercial setup NTEGRA Prima (NT-MDT). The setup was calibrated using commercial PZT (52/48) films (Inostek). Measurements were performed under an applied ac voltage with amplitude $V_{ac} = 2.5$ V and frequency $f = 50$ kHz. Piezoresponse versus dc voltage hysteresis loops [d_{33}^{eff} (V)] were measured in the pulse dc mode.[13] A commercial tip-cantilever Arrow Silicon SPM Sensor system (Nano World) was used. Magnetic properties of the samples were investigated with a SQUID magnetometer (MPMS-5; Quantum Design).

III. RESULTS AND DISCUSSION

A. Crystal structure

Figure 1(a) shows XRD data obtained at room temperature for an $x = 0.18$ compound prepared at 970 °C. The spectrum was collected from the flat of the pellet immediately after the synthesis. One can see that the XRD pattern can be fitted using a polar rhombohedral *R3c* model characteristic of pure $BiFeO_3$. Figure 1(b) demonstrates the XRD spectrum collected after 5 days of holding the pellet at room temperature. The pattern can be fit well using an antiferroelectric orthorhombic $PbZrO_3$-like model, previously successfully applied to $Bi_{0.85}Nd_{0.15}FeO_3$ ceramics.[4,5] It is important to note that the previous electron diffraction study of the orthorhombic phase showed that it has the *Pnam* structure, combining a complex $(a^-a^-c^+)/(a^-a^-c^-)$ octahedral tilting with antipolar displacements of A-site cations along the $[110/\bar{1}\bar{1}0]_c$ directions of the parent cubic perovskite cell.[4] However, it was also proven that this $NaNbO_3$-like tilting is not strong and/or sufficiently ordered to give clear superlattice reflections in conventional x-ray or neutron diffraction experiments.[4,5] Accordingly, the space group *Pbam* (combines $a^-a^-c^0$ octahedral tilting with antipolar displacements of A-site cations along the $[110/\bar{1}\bar{1}0]_c$ axis; the structure is characteristic of $PbZrO_3$ perovskite)[14] can be used in practice.[4,5] The primitive-cell volume for the

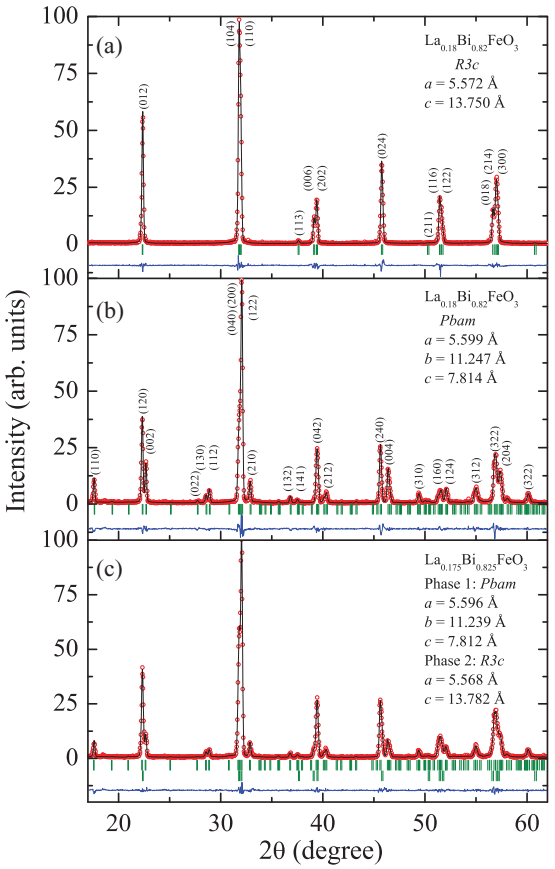

FIG. 1. (Color online) Observed, calculated, and difference XRD patterns obtained for $x = 0.18$ samples: (a) immediately after synthesis; (b) after 5 days at room temperature; and (c) obtained for relaxed samples, $x = 0.175$, and fitted in the two-phase model. Upper ticks denote *Pbam*; lower ticks, *R3c*.

Pbam lattice is about 0.2% smaller than that obtained for the *R3c* one. For an $x = 0.175$ compound, x-ray diffraction pattern obtained immediately after synthesis was satisfactorily fitted using the rhombohedral structural model. Holding the sample for 5 days at room temperature resulted in the appearance of a mixed structural state with a strongly dominant orthorhombic phase [Fig. 1(c)]. The roughly estimated phase ratio is 4:1. XRD measurements performed after 2 months did not reveal any structural changes. However, the initial rhombohedral phase became dominant (about 60%–70%) after annealing of both $x = 0.175$ and $x = 0.18$ samples at 350 °C for 1 h. The traces of the orthorhombic phase were still detected after 1 h of annealing at 600 °C, however, they completely disappeared after heat treatment for 10 h. Complete disappearance of the orthorhombic phase can also be achieved either via long-time annealing (20 h) at a moderate temperature (480 °C) or using short-time annealing (30 min) at 900 °C. A cool-down to 5 K has almost no effect on the phase ratio at room temperature. The rhombohedral structure of the $x = 0.16$ compound is stable under ambient conditions; no changes in x-ray diffraction patterns were detected during a 3-month control.

It is worth noting that the sample cooling rate does not affect the structural behavior: both quenched, from 350 ° to 970 °C, and slowly cooled (100 °C/h) samples have similar XRD patterns. However, both the duration and the temperature of the annealing are important: a higher temperature and longer duration of heat treatment favor a recovery of the rhombohedral phase at room temperature. Samples synthesized at a higher temperature and characterized by a larger average grain size demonstrate much faster structural transformation at room temperature, and complete isothermal transition into the orthorhombic phase can take only 1 day. So, one could suggest that the rearrangement and accumulation of structural defects during annealing and/or synthesis play an important role in the recovery of the rhombohedral lattice.

Somewhat different XRD results were obtained for the $x = 0.18$ sample ground into a powder immediately after synthesis. (Scanning electron microscopy measurements gave an average grain size of about 4 and 13 μm for powder and bulk samples, respectively.) For ground samples, traces of the *Pbam* phase (less than 5%) were detected. This powder was subjected to the low pressure of 0.2 GPa applied at room temperature for 5 min. The following XRD data confirmed the complete transformation into the *Pbam* phase. It is worth noting that this pressure value is comparable to the internal stresses typically occurring within ceramics.[15] The pressure-induced polar-antipolar (*R3c* to *Pbam*) phase transition has been observed in parent $BiFeO_3$ at a much higher pressure.[16] This transition is directly related to a smaller unit cell volume of the antipolar phase. The samples ground into a powder also exhibit an isothermal structural transition as well as complete recovery of the polar phase with annealing at 600 °C during 12 h. However, there is no evidence of a completed isothermal transition into the *Pbam* phase. Taking these facts into account, one could suggest that the strain/stress redistribution inside the grains (or strain relief) along with the structural defect rearrangement plays an important role also for the occurrence of isothermal structural transformation under ambient conditions. To our knowledge, this is the first

evidence of isothermal polar-antipolar structural transition for ceramics. Isothermal martensitic-like transitions have been reported earlier for many metallic alloys.[17]

Further increasing the lanthanum content hampers the formation of the rhombohedral phase. XRD data are in agreement with the assumption that compositions with $x > 0.20$ have an orthorhombic structure closely related to the antipolar $PbZrO_3$-type one. However, there are some changes in XRD pattern leading to poor resolution of some small superstructural diffraction peaks in the *Pbam* model. The basic perovskite peaks can be well described using a $\sqrt{2}a \times \sqrt{2}a \times 2a$ orthorhombic unit cell (a is the parameter of the cubic perovskite subcell), however, we failed to describe well all the peaks associated with antipolar displacements using a commensurate antipolar $\sqrt{2}a \times 2\sqrt{2}a \times 2a$ supercell. So, one could suggest that the basic orthorhombic symmetry is retained and some changes in XRD patterns are associated with the modulated antipolar ordering. This type of structure is preserved up to the $x = 0.45$ composition; intensities of the peaks associated with antipolar displacements decrease with increasing lanthanum content. The crystal structure of $x > 0.5$ compounds is well described with the nonpolar *Pnma* space group. Apparently, the change in antipolar order is the result of the high concentration of lanthanum ions that are polar-inactive and destabilize the commensurate antipolar order. It is probable that the crystal structure descriptions reported earlier[6,9–11] are associated with incorrect identification of the superstructure peaks as impurities and/or with a synthesis temperature that is too low, which could give rise to chemical inhomogeneity.

Results of the neutron diffraction measurements performed on samples crushed into a powder confirm the conclusions of the XRD data analysis. For the $x = 0.185$ compound (whose XRD measurement performed immediately after synthesis revealed an initially rhombohedral structure), NPD spectra were collected at 20 °, 240 °, 340 °, 420 °, and 700 °C. As expected, the room-temperature NPD data were reasonably well fitted using the antiferroelectric *Pbam* model. However, it was found that the agreement between experimental and calculated patterns could be improved by introducing an additional structural phase, *R3c*. Using a two-phase structural model allowed us to reduce χ^2 from 9.84 to 7.93, so we are inclined to think that the minor part (~7.5%) of the initial structural phase survived during the isothermal transformation. Increasing the temperature was found to change the phase ratio. A fraction of the rhombohedral phase rises to 10.5%, 24%, and 53% with an increase in temperature to 240 °, 340 °, and 420 °C, respectively, thus demonstrating a gradual antipolar-to-polar structural transformation upon thermal excitation. At 700 °C, the compound possesses a single-phase orthorhombic *Pnma* structure. Characteristic NPD patterns of the $x = 0.185$ compound are shown in Fig. 2. Structural data obtained by the Rietveld refinement of NPD spectra at selected temperatures are summarized in Table I.

Using of the two-phase model ($Pbam + R3c$) in the NPD refinement of the $x = 0.25$ sample at room temperature did not improve reliability factors of the fit in contrast to the $x = 0.185$ sample. For the single-phase *Pbam* model, the overall difference between observed and calculated profiles

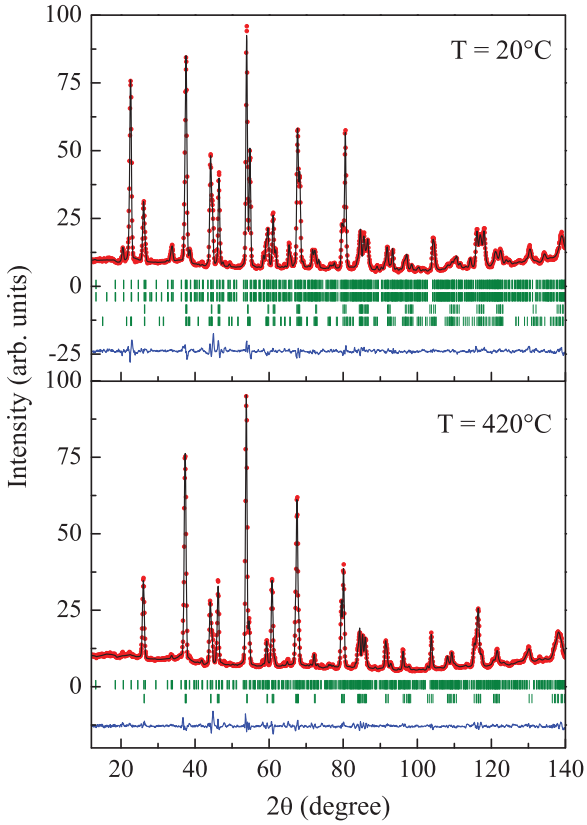

FIG. 2. (Color online) Observed (circles), calculated (solid line), and difference patterns resulting from Rietveld analysis of neutron powder diffraction data for the $x = 0.185$ sample obtained at 960 °C. Bragg reflections are indicated by tick marks.

was rather good as shown in Fig. 3; however, detailed verification of the fitting revealed the existence of several low-intensity peaks, which cannot be adequately fit by the mentioned model (see the insets in Fig. 3). Very similar NPD patterns were also collected at 220 °, 320 °, and 370 °C. Taking into account that the *Pbam* refinement describes very satisfactorily all the remaining peaks ($\chi^2 \sim 8$), we suppose that these unsolved low-intensity peaks may indicate an incommensurate structure, which can be described as a first approximation by a *Pbam* model with a commensurate subcell. It is necessary to emphasize that the unsolved low-intensity peaks cannot belong to any impurity phase: all these peaks disappear upon the temperature-induced transition to the *Pnma* phase, as confirmed by analysis of the spectra obtained at 470 ° and 700 °C. A precise determination of crystal structure of the low-temperature polymorph remains an open issue.

Taking into account all the data collected for $0.17 \leqslant x \leqslant 0.19$ compounds, one can state that the following sequence of transitions is realized upon cooling: the nonferroelectric orthorhombic phase *Pnma* transforms into the polar rhombohedral *R3c* and then to the antipolar orthorhombic *Pbam*. Both isothermal and thermal phase behavior can be understood by assuming that the energetic barrier between polar rhombohedral and antipolar orhorhombic phases is large, whereas the thermodynamic potentials (Gibbs free energy) are very close. So these phases can coexist or exist uniquely

TABLE I. Structural parameters for the $Bi_{0.815}La_{0.185}FeO_3$ compound obtained by Rietveld refinement of the NPD patterns collected at 20 °, 420 °, and 700 °C.

T (°C)	Model	Cell (Å)	Atom	Wyck	x	y	z	R factors (%)
20	*Pbam*	$a = 5.5896(1)$	Bi/La1	4g	0.706(2)	0.1236(9)	0	$R_p = 3.71$
	(92.5%)	$b = 11.2663(2)$	Bi/La2	4h	0.706(2)	0.1240(10)	0.5	$R_{wp} = 4.99$
		$c = 7.8020(1)$	Fe	8i	0.2393(7)	0.1268(5)	0.2487(12)	$R_{B1} = 6.27$
			O1	4g	0.292(2)	0.1515(13)	0	$R_{B2} = 5.01$
			O2	4h	0.294(2)	0.0837(11)	0.5	$R_{Bmag1} = 3.45$
			O3	8i	0.0380(13)	0.2615(8)	0.2821(9)	$R_{Bmag2} = 2.69$
			O4	4f	0	0.5	0.1887(14)	$\chi^2 = 7.93$
			O5	4e	0	0	0.219(2)	
	R3c	$a = 5.5663(10)$	Bi/La	6a	0	0	0	
	(7.5%)	$c = 13.7447(20)$	Fe	6a	0	0	0.226(2)	
			O	18b	0.467(4)	0.055(4)	0.967(3)	
420	*Pbam*	$a = 5.6297(4)$	Bi/La1	4g	0.735(5)	0.1367(20)	0	$R_p = 3.26$
	(47%)	$b = 11.2259(8)$	Bi/La2	4h	0.742(2)	0.1186(18)	0.5	$R_{wp} = 4.48$
		$c = 7.8354(3)$	Fe	8i	0.232(3)	0.1243(10)	0.2459(18)	$R_{B1} = 8.84$
			O1	4g	0.259(5)	0.169(4)	0	$R_{B2} = 2.28$
			O2	4h	0.273(4)	0.077(3)	0.5	$\chi^2 = 6.51$
			O3	8i	0.008(7)	0.242(3)	0.291(2)	
			O4	4f	0	0.5	0.203(4)	
			O5	4e	0	0	0.205(5)	
	R3c	$a = 5.591\,53(1)$	Bi/La	6a	0	0	0	
	(53%)	$c = 13.801\,03(1)$	Fe	6a	0	0	0.2277(5)	
			O	18b	0.4520(10)	0.0183(13)	0.9624(7)	
700	*Pnma*	$a = 5.6212(1)$	Bi/La	4c	0.0255(10)	0.25	0.9883(12)	$R_p = 2.97$
	(100%)	$b = 7.9290(2)$	Fe	4b	0	0	0.5	$R_{wp} = 4.57$
		$b = 5.5809(1)$	O1	4c	0.4853(15)	0.25	0.0764(14)	$R_B = 6.43$
			O2	8d	0.2095(9)	0.5345(8)	0.2148(10)	$\chi^2 = 6.78$

during a short window of time in a very wide temperature range. The isothermal transition between them occurs via the mechanism of inhomogeneous nucleation, which is strongly affected by temperature. The higher the temperature, the more effectively transition occurs, due to increasing mobility of the defects. At a higher temperature, the polar phase is more stable than the antipolar one, so an inverse isothermal transition takes place. One could suggest that the large energetic barrier between the two phases is associated with a low mobility of the lanthanum ions due to their relatively low polarizability. The rhombohedral polar phase becomes completely unstable at $x > 0.20$, where a modified type of the antipolar structure is observed.

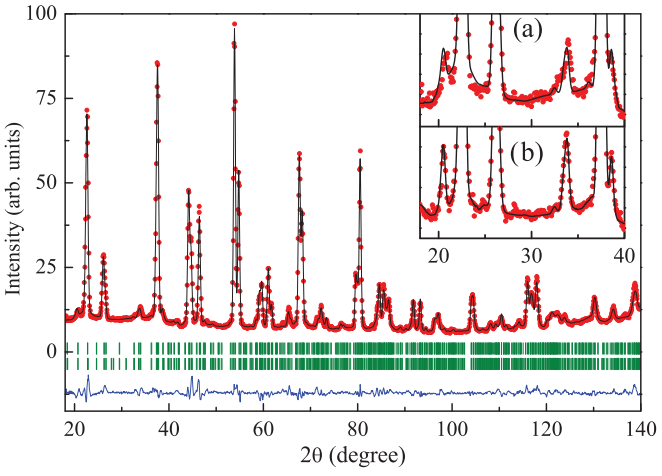

FIG. 3. (Color online) Observed (circles), calculated (solid line), and difference patterns resulting from Rietveld analysis of the neutron powder diffraction data for the $x = 0.25$ sample obtained at 990 °C. Bragg reflections are indicated by tick marks. Insets (a) and (b): Enlargement of part of the room-temperature experimental and calculated spectra obtained for $x = 0.25$ and $x = 0.185$ samples, respectively.

B. Magnetic properties

Figure 4(a) shows the field dependencies of the magnetization for $x = 0.16$, $x = 0.175$, and $x = 0.18$ samples at room temperature. The $x = 0.16$ sample is rhombohedral, whereas the relaxed sample with composition $x = 0.18$ has an orthorhombic (*Pbam*) structure. The $x = 0.175$ sample is in the intermediate stable structural state [Fig. 1(c)]. One can see that the rhombohedral sample exhibits a metamagnetic transition. This transition is associated with collapse of the spatially modulated antiferromagnetic structure.[8,9] In parent $BiFeO_3$, this transition appears in a magnetic field of about 14 T at room temperature.[9] In larger magnetic fields, a weakly ferromagnetic state is stabilized. The field dependencies of magnetization for $x = 0.175$ and $x = 0.18$ samples are typical of weak ferromagnets. However, the $x = 0.18$ compound possesses a spontaneous magnetization 20% larger than that obtained for the $x = 0.175$ sample. To understand the origin of the smaller magnetization of the $x = 0.175$ compound,

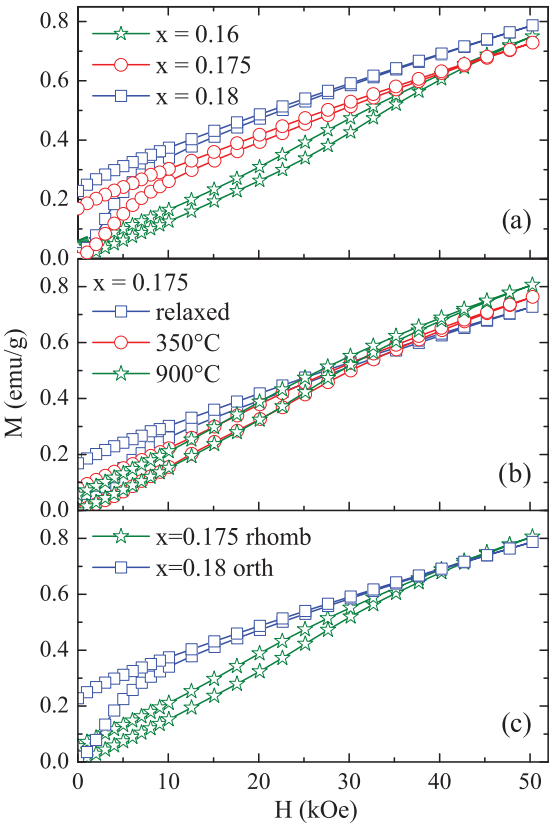

FIG. 4. (Color online) (a) Field dependence of the magnetization obtained for rhombohedral $x = 0.16$, relaxed $x = 0.175$, and orthorhombic $x = 0.18$ samples at room temperature. (b) Dependencies obtained for relaxed and annealed (1 h at 350 °C and 30 min at 900 °C) $x = 0.175$ samples. (c) tField dependencies of the magnetization for rhombohedral $x = 0.175$ and orthorhombic $x = 0.18$ compounds.

we annealed this sample at 350 ° and 900 °C and measured magnetization immediately after each annealing. A crossover from weakly ferromagnetic to antiferromagnetic behavior was observed [Fig. 4(b)]. It is worth nothing that the magnetization in a magnetic field of 5 T for the pure rhombohedral sample becomes equal to the magnetization of the pure orthorhombic $x = 0.18$ sample [Fig. 4(c)], in agreement with a completed metamagnetic transition into a weakly ferromagnetic state. Thus, we can explain the magnetization data assuming that the minor part of the initial sample does not exhibit either weak ferromagnetic or metamagnetic behavior, associated with *Pbam* and *R3c* phases, respectively. This means that the minor part of the relaxed $x = 0.175$ sample exhibits pure antiferromagnetic behavior associated with a change in the structural symmetry due to misfit strains at the interfaces between the phases. To our knowledge, this effect has not been reported previously for ceramic samples. The appreciable remanent magnetization observed for the pure polar phase $x = 0.175$ [Fig. 4(c)] apparently can be associated with material inhomogeneity (lattice defects, local variations of the chemical composition), which favors stabilization of the weak ferromagnetic phase in the absence of a magnetic field. So the polar $x = 0.175$ composition is at the concentration border of the antiferromagnet–weak ferromagnet transition within the polar structure. It is important to note that both the polar and the antipolar phases have the same magnetization in the weakly ferromagnetic state, thus demonstrating a similar origin of the canted magnetic structure for both phases [Fig. 4(c)]. The weak ferromagnetic state is a result of Dzyaloshinskii-Moriya interactions.[18] However, in $BiFeO_3$ the interplay between magnetoelectric and Dzyaloshinskii-Moriya interactions leads to the appearance of a modulated magnetic structure with zero spontaneous magnetization. An external magnetic field favors a weak ferromagnetic state, thus leading to metamagnetic behavior. Substitution of the bismuth ions with polar low-activity lanthanum ions leads to a decrease in off-centering distortion.[19] Apparently, this favors weak ferromagnetic state stabilization. However, the polar phase becomes structurally unstable before the pure weakly ferromagnetic state is realized within the polar phase.

C. Piezoelectric properties

Local piezoelectric loops have been measured in a broad range of applied bias voltage. Well-saturated local piezoresponse hysteresis loops were obtained for parent $BiFeO_3$ under the application of a maximum bias of 50 V [Fig. 5(a)]. Similar measurements were done in different parts of various

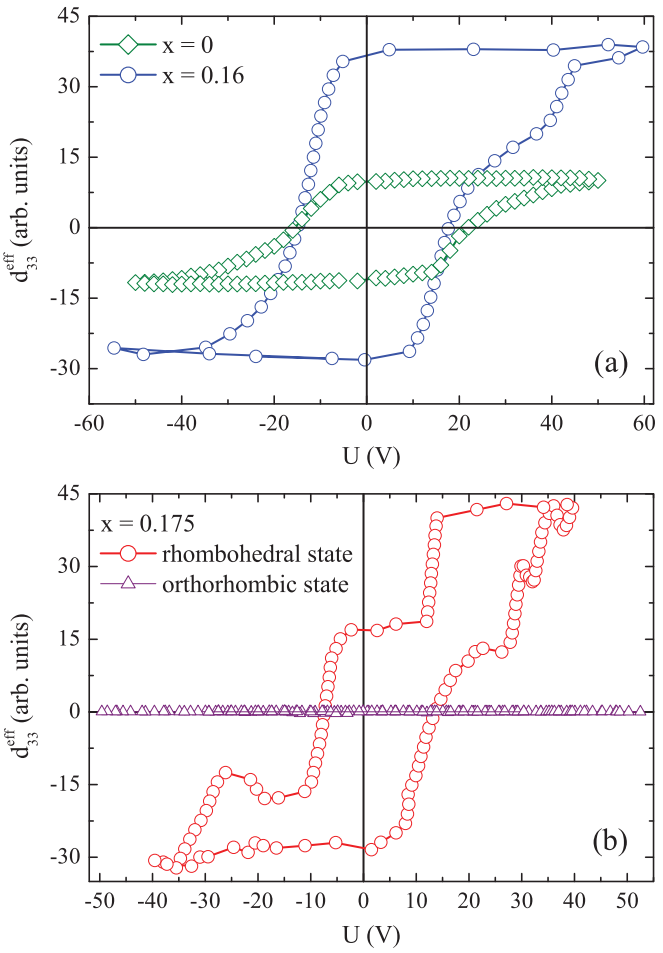

FIG. 5. (Color online) Typical room-temperature local piezoresponse loops for (a) rhombohedral $x = 0$ and $x = 0.16$ compounds and (b) $x = 0.175$ ceramics in rhombohedral and orthorhombic states.

granules, thus checking the effect of grain orientation and the possible contribution to electrostatic charges. Hysteresis loops of the piezoelectric coefficient were measured on the $x = 0.16$ compound using the same parameters as for the parent $BiFeO_3$ and the results demonstrated a more than threefold increase in the piezoresponse [Fig. 5(a)]. A slightly larger piezoresponse value (up to approximately 240 pm/V) was revealed for the $x = 0.175$ composition having a polar rhombohedral state. One from the measured local loops is presented in Fig. 5(b). The domain switching had a multiple step-like character. PFM measurements performed for the relaxed $x = 0.175$ composition showed vanishing switchable polarization in different parts of the sample [Fig. 5(b)]. However, PFM data obtained for the annealed sample containing about 60%–70% polar phase (roughly estimated from XRD data) displayed a clear piezoelectric response, which was strongly position dependent (Fig. 6). The hysteresis loops of the piezoelectric coefficient had the standard shape. All measurements were done using the same setup parameters. So the results displayed in Figs. 5 and 6 can be directly compared in magnitude. The magnitude of the piezoresponse for a mixed polar-antipolar state was less than that for the pure rhombohedral compositions. We failed to observe any piezoresponse associated with domain switching for the pure orthorhombic antipolar $x = 0.18$ compound. The macroscopic *P-E* dependencies for the antipolar compositions showed strongly linear behavior up to 100 kV/cm. It was shown earlier that thin films of composition $Bi_{0.8}La_{0.2}FeO_3$ exhibited a linear *P-E* dependence up to the field of 500 kV/cm.[20]

We suggest that the anomalous local hysteresis loops observed for the pure polar phase [Fig. 5(b)] could be caused by the domain wall pinning effect associated with charged defects. Double hysteresis loops due to the domain wall pinning effect were observed in the parent polar $BiFeO_3$.[21] The high stability of the antipolar phase in an external electric field seems to be related to the polar low-activity nature of lanthanum ions. Strong enhancement of the piezoresponse can be caused by the structural instability of the ferroelectric phase near the polar-antipolar phase boundary. Usually, a large piezoresponse is expected in the case where two different ferroelectric phases coexist. However, there are two different mechanisms of piezoelectric property enhancement.[22] The first mechanism is associated with polarization rotation, while the second is related to polarization extension, which is pronounced near the Curie point or polar-nonpolar morphotropic phase boundary.[22] So we can conclude that the enhancement of the piezoelectric properties in $Bi_{1-x}La_xFeO_3$ results from polarization extension occurring near the polar-antipolar morphotropic phase boundary. It was suggested[22] that the polarization extension mechanism may not fully develop near a polar-antipolar phase boundary because both phases have nonzero polarization on the unit cell scale. However, we have observed the largest piezoreponse in the uniform polar state. Our observation is similar to that for AlN doped with scandium, where a large piezoresponse was observed in the single-phase state and explained by structural competition and softening of the C_{33} elastic constant.[23]

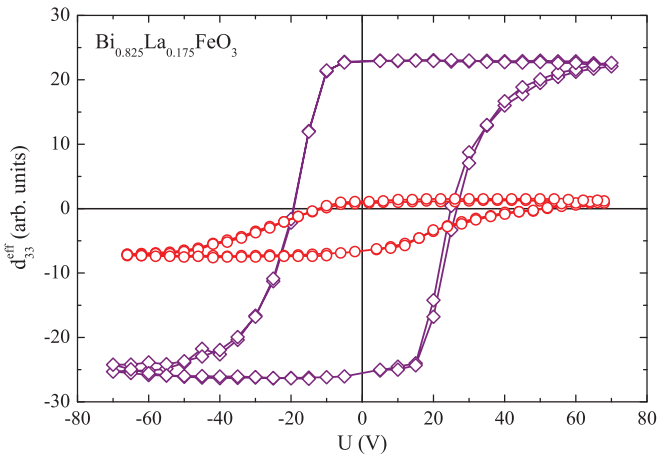

FIG. 6. (Color online) Local piezoresponse loops for $x = 0.175$ ceramics containing 60%–70% polar phase. Data were collected from different parts of the same grain.

IV. CONCLUSIONS

In summary, our results demonstrate that the initially rhombohedral polar structure of samples near the morphotropic phase boundary in $Bi_{1-x}La_xFeO_3$ ceramics gradually transforms into an antipolar orthorhombic structure at room temperature, whereas an inverse antipolar-polar transition is observed as the temperature rises above 300 °C. Both isothermal and thermal phase behavior can be understood by assuming that the energetic barrier between polar rhombohedral and antipolar orhorhombic phases is large, whereas the thermodynamic potentials (Gibbs free energies) are very close to each other. The polar-antipolar transition can also be induced under a low external pressure, but an electric-field-driven antipolar-polar transition is not observed in macroscopic measurements up to 100 kV/cm and local probe measurements by PFM. The crystal structure of $x > 0.20$ compositions is consistent with a modified antipolar order in comparison to compounds with a lower lanthanum content. The antipolar phase is characterized by a weak ferromagnetic state, whereas a polar phase at the morphotropic phase boundary was obtained in a mixed antiferromagnet-weak ferromagnet state. The mixed structural state possesses magnetic properties that are very different from those characteristic of the structurally uniform compositions. A structural instability of the polar phase at the morphotropic polar-antipolar phase boundary is responsible for the large piezoresponse, with a magnitude much greater than that for the initial $BiFeO_3$.

ACKNOWLEDGMENTS

The authors would like to acknowledge the financial support of the BRFFI (Grant Nos. T10R-119 and F09K-043), the Foundation for Science and Technology of Portugal (FCT) (the Ciência 2008 and Ciência 2007 programs and Grant No. SFRH/BPD/42506/2007). This research project has also been partly supported by the European Commission under the Seventh Framework Programme through the Key Action: Strengthening the European Research Area, Research Infrastructures [Contract No. 226507 (NMI3)].

*Corresponding author: troyan@physics.by

[1]G. Catalan and J. F. Scott, Adv. Mater. **21**, 2463 (2009).
[2]S. Fujino, M. Murakami, V. Anbusathaiah, S.-H. Lim, V. Nagarajan, C. J. Fennie, M. Wuttig, L. Salamanca-Riba, and I. Takeuchi, Appl. Phys. Lett. **92**, 202904 (2008).
[3]C.-J. Cheng, D. Kan, S.-H. Lim, W. R. McKenzie, P. R. Munroe, L. G. Salamanca-Riba, R. L. Withers, I. Takeuchi, and V. Nagarajan, Phys. Rev. B **80**, 014109 (2009).
[4]S. Karimi, I. M. Reaney, I. Levin, and I. Sterianou, Appl. Phys. Lett. **94**, 112903 (2009).
[5]I. Levin, S. Karimi, V. Provenzano, C. L. Dennis, H. Wu, T. P. Comyn, T. J. Stevenson, R. I. Smith, and I. M. Reaney, Phys. Rev. B **81**, 020103(R) (2010).
[6]S. Karimi, I. Reaney, Y. Han, J. Pokorny, and I. Sterianou, J. Mater. Sci. **44**, 5102 (2009).
[7]D. Kan, L. Pálová, V. Anbusathaiah, C. J. Cheng, S. Fujino, V. Nagarajan, K. M. Rabe, and I. Takeuchi, Adv. Funct. Mater. **20**, 1108 (2010).
[8]G. Le Bras, D. Colson, A. Forget, N. Genand-Riondet, R. Tourbot, and P. Bonville, Phys. Rev. B **80**, 134417 (2009).
[9]I. O. Troyanchuk, M. V. Bushinsky, D. V. Karpinsky, O. S. Mantytskaya, V. V. Fedotova, and O. I. Prochnenko, Phys. Status Solidi B **246**, 1901 (2009).
[10]S. T. Zhang, Y. Zhang, M.-H. Lu, C.-L. Du, Y.-F. Chen, Z.-G. Liu, Y.-Y. Zhu, N.-B. Ming, and X. Q. Pan, Appl. Phys. Lett. **88**, 162901 (2006).
[11]V. R. Singh, A. Garg, and D. C. Agrawal, Solid State Commun. **149**, 734 (2009).
[12]J. Rodriguez-Carvajal, Physica B **192**, 55 (1993).
[13]N. Balke, I. K. Bdikin, S. V. Kalinin, and A. L. Kholkin, J. Am. Ceram. Soc. **92**, 1629 (2009).
[14]A. M. Glazer, K. Roleder, and J. Dec, Acta Crystallogr., Sect. B: Struct. Sci. **49**, 846 (1993).
[15]G. Gogotsi, V. Galenko, B. Ozerskii, and N. Orlovskaya, Refract. Ind. Ceram. **42**, 341 (2001).
[16]A. A. Belik, H. Yusa, N. Hirao, Y. Ohishi, and E. Takayama-Muromachi, Chem. Mater. **21**, 3400 (2009).
[17]V. A. Lobodyuk and E. I. Estrin, Usp. Fiz. Nauk **175**, 745 (2005).
[18]C. Ederer and C. J. Fennie, J. Phys. Condens. Matter **20**, 434219 (2008).
[19]J.-H. Lee, H. J. Choi, D. Lee, M. G. Kim, C. W. Bark, S. Ryu, M.-A. Oak, and H. M. Jang, Phys. Rev. B **82**, 045113 (2010).
[20]Y. H. Chu, Q. Zhan, C.-H. Yang, M. P. Cruz, L. W. Martin, T. Zhao, P. Yu, R. Ramesh, P. T. Joseph, I. N. Lin, W. Tian, and D. G. Schlom, Appl. Phys. Lett. **92**, 102909 (2008).
[21]G. L. Yuan, Y. Yang, and S. W. Or, Appl. Phys. Lett. **91**, 122907 (2007).
[22]D. Damjanovic, Appl. Phys. Lett. **97**, 062906 (2010).
[23]F. Tasnadi, B. Alling, C. Höglund, G. Wingqvist, J. Birch, L. Hultman, and I. A. Abrikosov, Phys. Rev. Lett. **104**, 137601 (2010).